Supporting Material

Thick-to-thin filament surface distance modulates cross-bridge kinetics in Drosophila flight muscle

Bertrand C.W. Tanner[*], Gerrie P. Farman[†], Thomas C. Irving[‡],
David W. Maughan[*], Bradley M. Palmer[*], and Mark S. Miller[*]

* Department of Molecular Physiology and Biophysics, University of Vermont, Burlington, VT 05405. † Department of Physiology and Biophysics, Boston University, Boston, MA, 02118. ‡ Center for Synchrotron Radiation Research and Instrumentation, Department of Biological and Chemical Sciences, Illinois Institute of Technology, Chicago, IL 60616

Materials and Methods

Solutions: Solutions were prepared according to a computer program that solves the ionic equilibria (1). Concentrations are expressed in mmol/L (mM). Unless listed otherwise, all chemicals were purchased from Sigma-Aldrich (St. Louis, MO). Skinning solution was pCa 8.0 (pCa=-$\log_{10}[Ca^{2+}]$), 20 N,Nbis[2-hydroxyethyl]-2-aminoethanesulfonic acid (BES), 10 DTT, 5 EGTA, 1 Mg^{2+}, 5 MgATP, 0.25 P_i, protease inhibitor cocktail (Roche; Indianapolis, IN), ionic strength of 175 mEq adjusted with sodium methane sulfate, pH 7.0, with 50% w/v glycerol subsequently added and 0.5% Triton X-100. Storage solution was skinning solution without Triton. For x-ray diffraction measurements, relaxing solution was pCa 8.0, 20 BES, 15 creatine phosphate (CP), 300 U/mL creatine phosphokinase (CPK), 1 DTT, 5 EGTA, 1 Mg^{2+}, 15 MgATP, 8 P_i, ionic strength of 200 mEq adjusted with sodium methane sulfate at pH 7.0. For mechanics experiments, activating solution was pCa 4.0, 20 BES, 20 CP, 450 U/mL CPK, 1 DTT, 5 EGTA, 1 Mg^{2+}, 12 MgATP, 2 P_i, 200 mEq ionic strength, pH 7.0; and relaxing solution (used during fiber mounting) was same as activating solution except at pCa 8.0.

X-ray diffraction: Single dorsolongitudinal muscle fibers were isolated from thoraces of 2-3 day old female flies, demembranated in skinning solution for 1 hour at 4°C, clipped with aluminum T-clips, and transferred to storage solution at -20˚C until use. Within five days of dissection, fibers were transferred from storage solution to perfusion chambers filled with relaxing solution (0% Dextran) and secured between adjustable hooks. Fibers were visually stretched beyond just taut to approximate the fiber lengths used during mechanics experiments and placed in the path of the x-ray beam. Perfusion chambers had thin Mylar windows allowing x-rays to pass through the fibers and transmural ports allowing solution exchanges via syringe. The peak intensity, widths, and separations for the 1,0 and 2,0 equatorial reflections were estimated using a non-linear least squares fitting procedure (2). The separation of the 1,0 equatorial reflections was transformed into the distance between the lattice planes of the thick filaments ($d_{1,0}$), which was converted to center-to-center distance between thick filaments (= $d_{1,0} \times 2/\sqrt{3}$), yielding inter-thick filament spacing.

Muscle mechanics: Single IFM fibers were dissected and skinned as described above for x-ray diffraction measurements, split lengthwise to ~100 μm diameter to reduce the cross-sectional area, clipped with aluminum T-clips, lowered into relaxing solution, then mounted between a

silicon crystal strain gauge and piezoelectric motor. Fibers were stretched 5% from their just-taut length in 1% increments, waiting 1 minute between each stretch, activated to pCa 4.5 in the absence of Dextran, and stretched in 3% increments until oscillatory work production reached a stable maximum as measured via sinusoidal analysis. Following each 3% stretch, we waited 3-5 minutes for tension to relax and stabilize before applying the sinusoidal analysis. This protocol was required to accommodate the high stiffness and a relatively large contribution of passive tension to total active tension in IFM fibers (3). Activating solutions with increasing Dextran concentrations were exchanged to obtain 4 and 6% T-500 or 0.34, 0.78, 10, and 20% T-10. Following each activating solution change, fibers were shortened until slack, allowed to equilibrate for 5 minutes, then re-stretched until oscillatory work reached a stable maximum.

Statistical Analysis: To examine statistical trends among Dextran T-500 or T-10 measurements we applied a repeated-measures analysis with Dextran concentration as the repeated measure, followed by a Bonferroni adjusted pair-wise comparison of the means at each Dextran concentration. To examine inter-Dextran statistical differences between all measurements we applied a one-way ANOVA followed by a Tukey-Kramer multiple comparison of the means.

Discussion

Using electron density maps and myofilament lattice models of skinned skeletal muscle from frogs, Irving and Millman (2) showed that both myofilament lattice spacing and thick filament diameter decreased proportionally at modest osmotic pressures (0-3 kPa). Thus, we used a 1:1 ratio for thick filament compression to myofilament lattice compression to derive our structural model (Fig. 4). However, the stiffer thick filaments of fruit fly IFM may resist compression more than thick filament backbones of frog skeletal muscle, suggesting that a different compression ratio (*i.e.* <1:1) may be more appropriate for fly flight muscle.

To investigate the sensitivity of our structural model to different ratios of thick filament backbone compression with respect to myofilament lattice spacing compression, we reduced the effect of osmotic compression on thick filament radii (r_{thick}) by 1/2 (Fig. S1 A and C) and 1/4 (Fig. S1 B and D), without changing the effect of osmotic compression on the measured myofilament lattice spacing. These changes in the compression ratio value had a small effect, shifting 0% Dextran values to slightly larger distances for compression ratios of 0.5:1 (Fig. S1 A and C) to 0.25:1 (Fig. S1 B and D). There were no changes in the in vivo r_{thick} values at 4% T-500 and 0.34% T-10, as expected. For 6% T-500 and 0.78% T-10, these compression ratios shifted thick-to-thin filament surface distance to slightly smaller values. Across all these models, the relationships between cross-bridge kinetics and thick-to-thin filament surface distance varied, but maintained the important trends that T-10 increased and T-500 decreased thick-to-thin filament surface distance. Altogether, these results show that the structural model is relatively insensitive to the exact value chosen for the compression ratio between the thick filament backbone and the myofilament lattice as a whole.

Our findings that thick-to-thin filament surface distance dictates the rates of cross-bridge force development and detachment arise from the primary assumption that the thick filament radius (r_{thick}) decreases proportional to osmotic pressure, whether produced by T-500 or T-10. However, it remains possible that Dextran T-500 and T-10 could reduce thick filament backbone

dimensions differently at matched osmotic pressures. Therefore, we recast the model to illustrate a range of possibilities where T-500 and T-10 differentially affect thick filament backbone compression (Fig. S2). However, for this set of plots we assumed that skinning results in the same value for r_{thick} (*i.e.* starting from 8.8 nm at 0% Dextran for T-500 and T-10). This is a slightly different assumption than the assumption applied to the data of Fig. S1, where osmotic pressure had differential effects on thick filament backbone compression versus myofilament lattice compression. Fig. S2 illustrates that our primarily findings hold across a range of differential compression possibilities for T-500 and T-10, including the subset explored in Fig. S1. Specifically, t_{on} correlates with thick-to-thin filament surface distance for all T-500 compression ratios, including no thick filament compression (0:1 compression ratio). t_{on} correlates with thick-to-thin filament surface distance for any T-10 compression ratio greater than 0.15:1, the ratio that predicts a vertical line for t_{on} versus thick-to-thin filament surface distance.

References

1. Godt, R. E. and B. D. Lindley. 1982. Influence of temperature upon contractile activation and isometric force production in mechanically skinned muscle fibers of the frog. *J. Gen. Physiol.* 80:279–297.

2. Irving, T. C. and B. M. Millman. 1989. Changes in thick filament structure during compression of the filament lattice in relaxed frog sartorius muscle. *J. Muscle Res. Cell Motil.* 10:385–394.

3. White, D. C. 1983. The elasticity of relaxed insect fibrillar flight muscle. *J. Physiol.* 343:31–57.

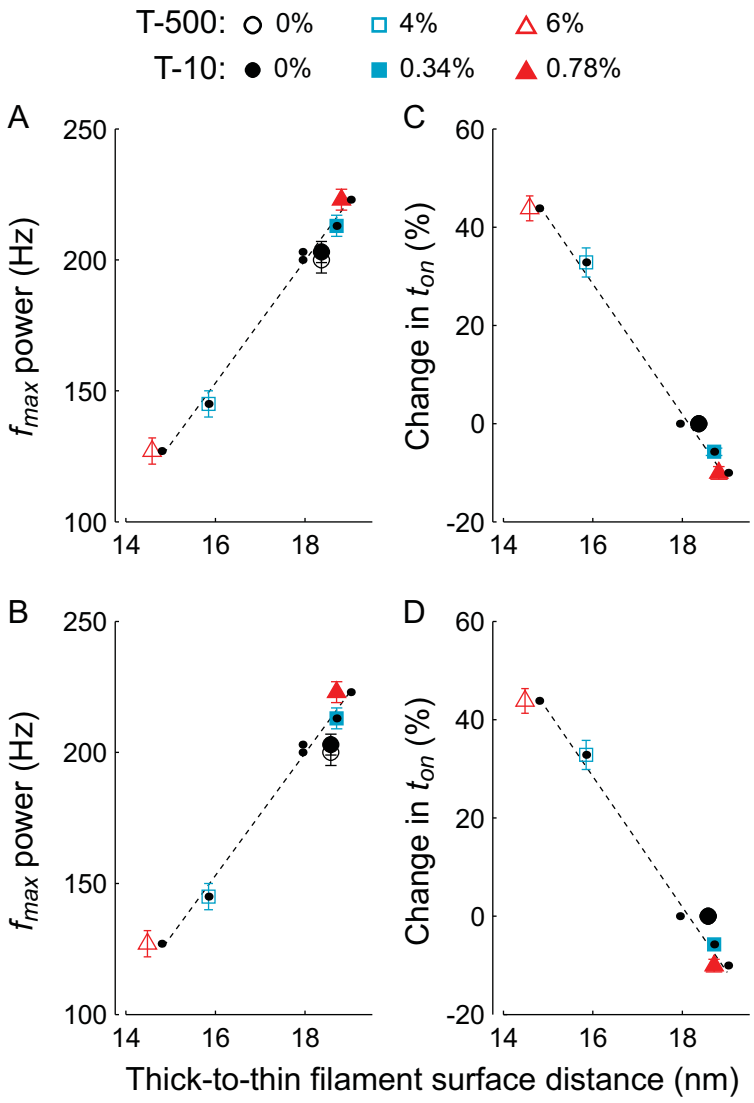

Figure S1: Frequency of maximal power (A and B) and myosin attachment time (C and D) are plotted against modeled thick-to-thin filament surface distance for thick filament backbone to myofilament compression ratios of 0.5:1 (A and C) and 0.25:1 (B and D). For reference, mean data and linear fits to the mean data from Fig. 5 are plotted as black dots and dashed lines to illustrate the 1:1 thick filament backbone to myofilament compression ratio presented in the main manuscript.

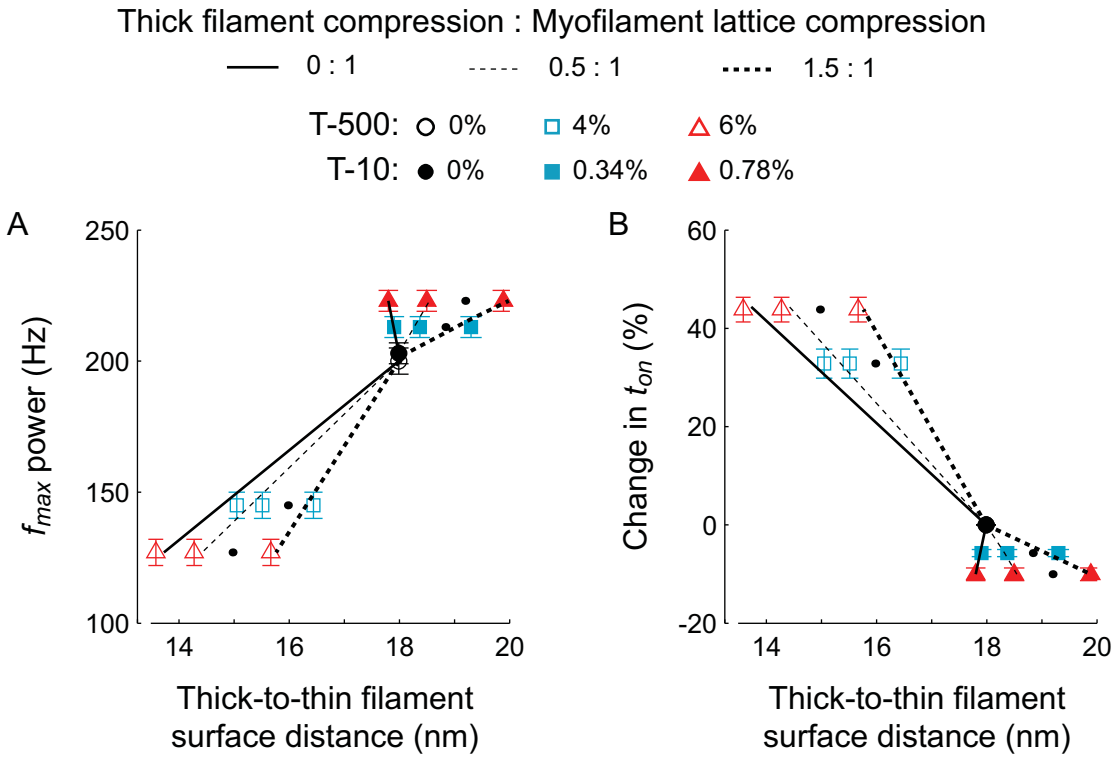

Figure S2: Frequency of maximal power (A) and change in myosin attachment time (B) are plotted against modeled thick-to-thin filament surface distance for conditions where i) T-500 and T-10 do not re-compress the thick filament backbone from the 0% Dextran condition (0:1 compression ratio), ii) Dextran T-500 and T-10 re-compress the thick filament backbone 50% less than the myofilament lattice (0.5:1 compression ratio), and iii) Dextran T-500 and T-10 re-compress the thick filament backbone 50% more than myofilament lattice (1.5:1 compression ratio). For reference, mean data from Fig. 5 are plotted as black dots to illustrate the 1:1 thick filament backbone to myofilament compression ratio presented in the main manuscript.